Reduced Order Modeling for Feedback Control of a Flexible Wing at Low Reynolds Numbers

M. Nardini, S. C. Schlanderer, R. D. Sandberg, S. J. Illingworth

Department of Mechanical Engineering
University of Melbourne, Parkville, Victoria 3010, Australia

Abstract

A variety of unsteady aerodynamic models for a two-dimensional rigid plate undergoing pitching and plunging motion is present in the literature. For a two-dimensional flexible wing, unsteady forces are generated by the wing deflection in time. Hence the necessity of unsteady models that also take into account the flexible degrees of freedom of the wing. In the present work, the deflection of a flexible wing immersed in a uniform free-stream has been decomposed using a truncated Fourier series. The effects of a prescribed deflection of the flexible wing on the flowfield in terms of each one of the leading modes (from 1 to 10) have been investigated using high-fidelity Direct Numerical Simulation (DNS) for viscous, compressible flows at low Reynolds numbers. System identification techniques are applied to obtain reduced order state-space models that relate the deflection of the wing to the measured lift. The system identification procedure is presented and the accuracy and validity of the reduced order models are discussed. Finally, the characteristics and the performance of the reduced order models are addressed from a feedback control point of view.

Introduction

Micro-Air Vehicles (MAVs) are a class of unmanned aerial vehicles characterized by reduced dimensions. Due to their reduced size, the inertia forces are of the same order of magnitude as the aerodynamic loads and thus the flight dynamic time scales and the aerodynamic time scales are comparable. This allows MAVs to perform strict and agile maneuvers that are impracticable for larger air vehicles. On the other hand, their reduced size makes MAVs sensitive to disturbances such as gusts. As the size of air vehicles decreases, unsteady aerodynamic effects will play a pivotal role in enabling fast maneuvers and responding to disturbances [12].

As observed in many natural flyers (i.e. bats), most wings are not rigid and their shape constantly changes during flight, significantly improving aerodynamic performance [6]. Therefore, a flexible wing is one solution that can be applied to MAVs in order to improve their maneuvrability and controllability.

The aim of this work is to investigate how the lift of a flexible wing is affected by a prescribed deflection. A two-dimensional low-thickness flexible wing, when modeled as a continuum, has an infinite number of degrees of freedom; to make the problem tractable, the wing's deflection is decomposed into its Fourier components, truncating the infinite sum to take into account only the leading Fourier modes. We will see that the largest unsteady forces are generated by the first few Fourier modes, with the contribution decreasing for increasing mode number, thus justifying this approach.

DNS is a powerful tool to investigate the unsteady aerodynamics of a flexible wing at low Reynolds numbers. However, despite the increasing computational capabilities of modern computers, DNS can be computationally expensive and does not provide insights on the characteristics of a fluid system that are important for its feedback control. Hence there is need of a reduced order model that is able to preserve the accuracy of the DNS, significantly reducing the computational cost, but that is also compatible with modern control techniques.

Unsteady Aerodynamic Model

The present work follows the procedure presented by Brunton in [2]: details of the procedure, briefly summarized here, can be found in the reference, together with an overview on unsteady aerodynamic models.

A general model of a physical system, indicating the state vector of the system with $\mathbf{x}$, the input vector with $\mathbf{u}$, the output vector with $\mathbf{y}$ and a set of parameters related to the physics of the system with μ, can be written as:

$$\dot{\mathbf{x}} = \mathbf{f}(\mathbf{x}, \mathbf{u}, \mu)$$
$$\mathbf{y} = \mathbf{g}(\mathbf{x}, \mathbf{u}, \mu), \tag{1}$$

where $\mathbf{f}$ and $\mathbf{g}$ are generic non-linear functions used to model the physical system.

For the specific case of a pitching flat plate, equation (1) can be expressed as

$$\dot{\mathbf{x}} \triangleq \frac{d}{dt} \begin{bmatrix} \mathbf{x} \\ \alpha \\ \dot{\alpha} \end{bmatrix} = \begin{bmatrix} f_{NS}(\mathbf{x}, \alpha, \dot{\alpha}, \ddot{\alpha}) \\ \alpha \\ \dot{\alpha} \end{bmatrix} \tag{2}$$
$$y = g_{lift}(\mathbf{x}, \alpha, \dot{\alpha}, \ddot{\alpha}).$$

α, $\dot{\alpha}$ and $\ddot{\alpha}$ represent the angle of attack and its first and second time derivatives respectively, while f_{NS} and g_{lift} are related to the non-linear Navier-Stokes equations. The superscript dot will be used from now on to indicate time derivatives.

Brunton introduced a state-space reduced order model based on the linearization of the two-dimensional, unsteady, incompressible Navier-Stokes equations around an equilibrium condition for a rigid flat plate. The equilibrium condition is defined by the base angle of attack α_0 and by the choice of the parameters μ, which include the Reynolds number and the pitching axis location. In a linear state-space form, if $\mathbf{x}$ represents the vorticity of the fluid, equation (2) becomes

$$\frac{d}{dt} \begin{bmatrix} \mathbf{x} \\ \alpha \\ \dot{\alpha} \end{bmatrix} = \begin{bmatrix} \mathbf{A} & \mathbf{0} & \mathbf{0} \\ \mathbf{0} & 0 & 1 \\ \mathbf{0} & 0 & 0 \end{bmatrix} \begin{bmatrix} \mathbf{x} \\ \alpha \\ \dot{\alpha} \end{bmatrix} + \begin{bmatrix} \mathbf{B} \\ 0 \\ 1 \end{bmatrix} \ddot{\alpha}$$
$$C_L = \begin{bmatrix} \mathbf{C} & C_\alpha & C_{\dot{\alpha}} \end{bmatrix} \begin{bmatrix} \mathbf{x} \\ \alpha \\ \dot{\alpha} \end{bmatrix} + C_{\ddot{\alpha}} \ddot{\alpha}. \tag{3}$$

C_L indicates the two-dimensional lift coefficient defined as $C_L = 2L/\rho U^2 c$, where L is the lift, ρ the fluid density of the undisturbed flow, U the free-stream velocity and c the wing chord. C_α is defined as $C_\alpha = \partial C_L / \partial \alpha$ and similarly $C_{\dot{\alpha}} = \partial C_L / \partial \dot{\alpha}$ and $C_{\ddot{\alpha}} = \partial C_L / \partial \ddot{\alpha}$. The following definitions follow: $\mathbf{A} = \partial f_{NS} / \partial \mathbf{x}$, $\mathbf{B} = \partial f_{NS} / \partial \ddot{\alpha}$ and $\mathbf{C} = \partial g_{lift} / \partial \mathbf{x}$. From equation (2), a model for plunging can also be obtained by simply changing the input of the system from pitching acceleration to plunging acceleration [2]. Pitching and plunging can also be combined in a multi-input single-output system [1].

In the present work, the procedure introduced by Brunton is extended to take into account the deflection of a two-dimensional wing. The deflection in time $w(x,t)$ of the mean line of the wing can be expressed using a truncated Fourier series:

$$w(x,t) = \sum_{k=1}^{N} \mathcal{W}_k(t) \cdot \sin\left(\frac{k\pi x}{c}\right), \text{ for } x \in [0,c], \quad (4)$$

where c represents the wing chord, k the deflection mode, $\mathcal{W}_k(t)$ the amplitude of the deflection related to the k-th mode and N the global number of modes taken into account. In analogy with equation (3), for each deflection mode k, the following coefficients can be defined $C_{\mathcal{W}_k} = \partial C_L / \partial \mathcal{W}_k$, $C_{\dot{\mathcal{W}}_k} = \partial C_L / \partial \dot{\mathcal{W}}_k$ and $C_{\ddot{\mathcal{W}}_k} = \partial C_L / \partial \ddot{\mathcal{W}}_k$. Consequently, the following relations hold:

$$\frac{d}{dt}\begin{bmatrix} \mathbf{x_k} \\ \mathcal{W}_k \\ \dot{\mathcal{W}}_k \end{bmatrix} = \begin{bmatrix} \mathbf{A_k} & \mathbf{0} & \mathbf{0} \\ \mathbf{0} & 0 & 1 \\ \mathbf{0} & 0 & 0 \end{bmatrix}\begin{bmatrix} \mathbf{x_k} \\ \mathcal{W}_k \\ \dot{\mathcal{W}}_k \end{bmatrix} + \begin{bmatrix} \mathbf{B_k} \\ 0 \\ 1 \end{bmatrix}\ddot{\mathcal{W}}_k$$

$$C_L^k = \begin{bmatrix} \mathbf{C_k} & C_{\mathcal{W}_k} & C_{\dot{\mathcal{W}}_k} \end{bmatrix}\begin{bmatrix} \mathbf{x_k} \\ \mathcal{W}_k \\ \dot{\mathcal{W}}_k \end{bmatrix} + C_{\ddot{\mathcal{W}}_k}\ddot{\mathcal{W}}_k. \quad (5)$$

C_L^k represents the lift generated by a deflection in the single k-th mode. The global lift due to all the considered modes can be reconstructed by simply adding together the single contributions from each mode (i.e. simple superimposition). The contributions of pitching and plunging can also be included.

System Identification

An approximation of the model is obtained from DNS through system identification and model reduction techniques. The aim of the procedure is to identify the values of the coefficients $C_{\mathcal{W}_k}$, $C_{\dot{\mathcal{W}}_k}$ and $C_{\ddot{\mathcal{W}}_k}$ (quasi-steady and added-mass force coefficients) from a lift pulse response generated via DNS and to find a low order approximation of the matrices $\mathbf{A}$, $\mathbf{B}$ and $\mathbf{C}$ representing the transient dynamics. Matrices and coefficients of each model depend on parameters such as the wing shape, the Reynolds number and the equilibrium condition chosen to linearize the Navier-Stokes equations. A deflection velocity pulse for a single mode k is applied to the wing and the response in terms of lift is obtained from the DNS. The lift coefficient for quasi-steady lift and added-mass are identified and subtracted from the pulse response. The remaining signal is used to derive a low order approximation of $\mathbf{A}$, $\mathbf{B}$ and $\mathbf{C}$. This is achieved using the Eigensystem Realization Algorithm (ERA), introduced in [5]. The model obtained using ERA is equivalent to a model obtained by Balanced Proper Orthogonal Decomposition, as demonstrated in [9]. The entire identification procedure for a pitching plate is explained in detail in [2] and it can be similarly extended to the flexible modes of the present wing, simply assuming a model in the form of equation (5).

The procedure introduced in [2] is based on pulse responses obtained using an incompressible code. In the present work, a compressible code is used, introducing the Mach number M as an additional parameter. Hence the reduced order model also depends on the Mach number. More importantly, compressibility has an effect on the pulse response, affecting the high frequencies. In particular, compressiblity introduces a phase lag between the acceleration (input) and the high-frequency lift response. In a compressible formulation there is no direct proportionality between acceleration and lift, as is the case in an incompressible formulation. However, the models presented in equations (3-5) can also be applied to compressible flows: the main difference is that in the compressible formulation the

high-frequency added-mass, instead of being captured by the coefficients $C_{\ddot{\alpha}}$ and $C_{\ddot{\mathcal{W}}_k}$, is included in the model as a transient.

Maneuvers

The maneuvers used for system identification and for the validation of the reduced order models are presented in this Section.

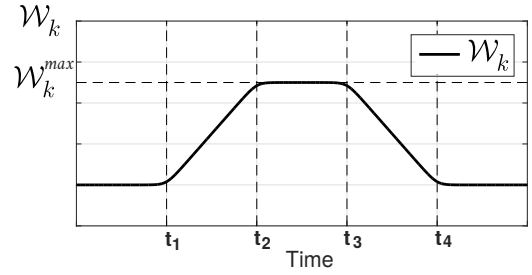### Canonical Ramp-up, Hold, Ramp-down Maneuver

Figure 1: Canonical ramp-up, hold, ramp-down maneuver. The deflection of generic mode k is shown and the four time corners of the maneuver are highlighted.

The following maneuver, used as a benchmark to compare the performance of the reduced order model with the results from DNS, is based on the pitch-up, hold and pitch-down maneuver introduced by the AIAA fluid dynamics technical committee on low-Reynolds number aerodynamics discussion group [3]. Here the angle of attack is simply replaced by the amplitude of the deflection in the k-th mode $\mathcal{W}_k$:

$$\mathcal{W}_k(t) = \mathcal{W}_k^{max}\frac{G(t)}{\max(G(t))}$$

$$G(t) = \log\left[\frac{\cosh(a(t-t_1))\cosh(a(t-t_4))}{\cosh(a(t-t_2))\cosh(a(t-t_3))}\right]. \quad (6)$$

$\mathcal{W}_k^{max}$ represents the maximum value of the deflection reached during the maneuver and a determines how gradual the maneuver is (determining the magnitude of the acceleration and the sharpness of the corners at t_1, t_2, t_3 and t_4). t_1, t_2, t_3 and t_4 define the time boundaries of the various phases of the maneuver, as shown in figure (1), and they correspond to the position in time of the peaks of the acceleration.

System Identification - Linear Ramp Maneuver

The following maneuver has been introduced by Brunton in [2] and it is obtained from the maneuver introduced in the previous section, simply isolating the ramp-up portion. t_1 and t_2 represent the boundaries of the ramp-up portion. This maneuver is used to approximate a pulse in the deflection velocity of the flexible wing and to obtain the pulse lift response necessary for system identification through ERA. Equation (7) shows the analytical expression of the maneuver.

$$\mathcal{W}_k(t) = \mathcal{W}_k^{max}\frac{G(t)}{\max(G(t))}$$

$$G(t) = \log\left[\frac{\cosh(a(t-t_1))\cosh(-a(t_2))}{\cosh(a(t-t_2))\cosh(-a(t_1))}\right] \quad (7)$$

Direct Numerical Simulations

Numerical simulations are carried out using a well-validated DNS code for compressible, viscous flows. The geometry of the flexible wing immersed in the flow and the consequent no-slip boundary condition are represented by a Boundary Data Immersion Method (BDIM) [10]. The code and the

BDIM method have been rigorously validated on a number of example problems, including the two-dimensional flow around a cylinder at $Re = 100$ [11] and the flow around a membrane at low and moderate Reynolds numbers [4].

Simulation Setup

For the present study, a two-dimensional flexible wing of unit length ($c = 1$) and constant 0.9% thickness is immersed in a uniform free-stream at zero angle of attack and $Re = 100$. The Reynolds number is defined as $Re = Uc/\nu$, where U is the free stream velocity, c is the chord length of the wing and ν the kinematic viscosity of the fluid.

The deflection in time for each single mode of the flexible wing is prescribed and it represents an input to the simulation. A grid convergence study has been performed in order to determine the size of the fluid domain and the grid resolution that guarantees grid-independent results. The grid is an Eulerian Cartesian grid of dimensions $60c \times 60c$, with a resolution of 409×460 grid cells. The grid is refined in the vicinity of the wing and the minimum grid spacing in both directions is $\Delta x = \Delta y = 1 \times 10^{-3}$. In the x-direction, the grid is refined towards the leading and trailing edges.

The leading and trailing edges are represented as sharp edges. Additional simulations performed with round edges did not show significant differences in the global measured lift for the Reynolds number considered.

Mach Number

For steady and quasi-steady simulations, flows with low Mach numbers ($M << 1$) can be treated as if they were incompressible. Unsteady flows might show significant compressibility effects if the frequencies are high relative to the speed of sound, even if the Mach number is low. Considering an oscillating flat plate with reduced frequency $\omega_r = \frac{\omega c}{U}$, where ω is the pulsation of the oscillations, the assumption of incompressible flow can be justified only if, in addition to $M << 1$, $M\omega_r << 1$ also holds [7]. Compressiblity effects change the amplitude and phase of the lift response to an unsteady motion, compared to the incompressible case [8].

Because pressure waves generated by an unsteady maneuver are traveling at a finite speed, in the presence of high accelerations (such as the linear ramp used for system identification) the response of the lift strongly depends on the Mach number [8]. Consequently, referring to equation (1), in a compressible code the Mach number must be included in the parameter μ. In the limit of $M \rightarrow 0$, the incompressible solution is recovered. It is beyond the scope of this work to fully characterize the effects of the Mach number on the lift response of an unsteady maneuver. For the present study, $M = 0.2$ is chosen as the Mach number for the system identification procedure.

Pulse Responses

The responses of the lift to a deflection velocity pulse in mode 1 and mode 2 are shown in figure (2). The pulse has the form of equation (7): the duration of the pulse is $\tau_2 - \tau_1 = 0.001$, to adequately identify the high frequency in the model. τ indicates dimensionless convective time $\tau = tU/c$. The parameter a is set to 1000 and the maximum deflection is $\mathcal{W}_1^{max} = \mathcal{W}_2^{max} = 0.0017453$, where the subscripts 1 and 2 refer to mode 1 and 2 respectively.

Two different scales are used to adequately represent the pulse responses. The first part of the pulse (high frequencies) is related to the acceleration of the deflection. Pressure waves are generated on the wing surface, traveling at the speed of sound. The time-scale of the first part of the response is strictly re-
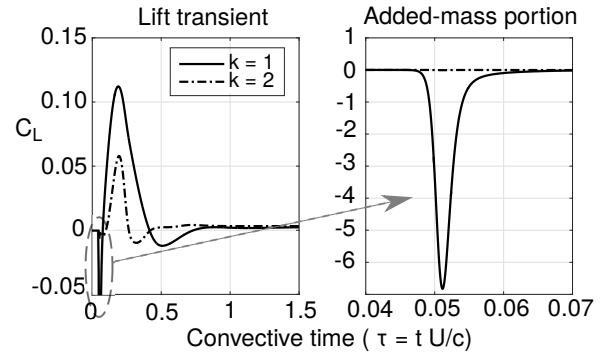

Figure 2: Pulse response for mode 1 and mode 2. Two different time-scales are used to show the rapid acceleration response and the slower consequent transient. After the transient, a steady-state is reached (not shown in the figure).

lated to the duration of the pulse. The fast acceleration-related response is followed by a slower transient, before the system reaches a steady-state. The steady-state for both modes has been omitted from figure (2). The pulse responses shown in figure (2) are used to generate a reduced order model in the form of equation (5) for each mode. Increasing the mode number k, the magnitude of the lift response decreases for both even and odd modes.

Mode 1 and odd modes in general show a significant peak in the lift response: a positive deflection causes higher pressure on the wing upper surface and lower pressure on the lower surface, resulting in a global lift that has opposite sign to the deflection itself. The high-frequency lift response has opposite sign compared to the steady-state lift. This leads to limitations in the performance of a closed-loop controller because of the inverse response.

Mode 2 and even modes generate a pulse response orders of magnitude smaller than that of even modes. The shape of the deflection generates higher pressure and lower pressure regions equally on both upper and lower surfaces, resulting in a global lift close to zero. This behavior is of fundamental importance from a control point of view: the smaller high-frequency response of the even modes can be seen as a time delay, posing significant limitations on the performance of any feedback controller designed for the system, because actuation has an effect only after waiting a certain time $\bar{\tau}$.

Validation and Model Performance

Figure (3) shows the frequency response for magnitude and phase (Bode plot) of the reduced order models obtained for modes 1 and 2. DNS was performed with the flexible wing deflecting at prescribed frequencies to validate the model. The magnitude and phase difference between the prescribed acceleration (sinusoidal input) and the output (lift) are evaluated and the results are compared with those from the reduced order models, showing excellent agreement in the considered frequency range.

A generic deflection of the wing is prescribed using a combination in time and space of modes 1 to 3, as shown in figure (4). The deflection of each mode is prescribed using the ramp-up, hold, ramp-down maneuver in equation (6). For each mode $a = 11$, while the other parameters can be inferred from figure (4). The lift from DNS is compared to the output of the reduced order model. All the unsteady effects are well captured by the reduced order model and minor differences can be noticed only where the wing deflection is highest, probably due to small non-linearities in the flow. In figure (4) the shape
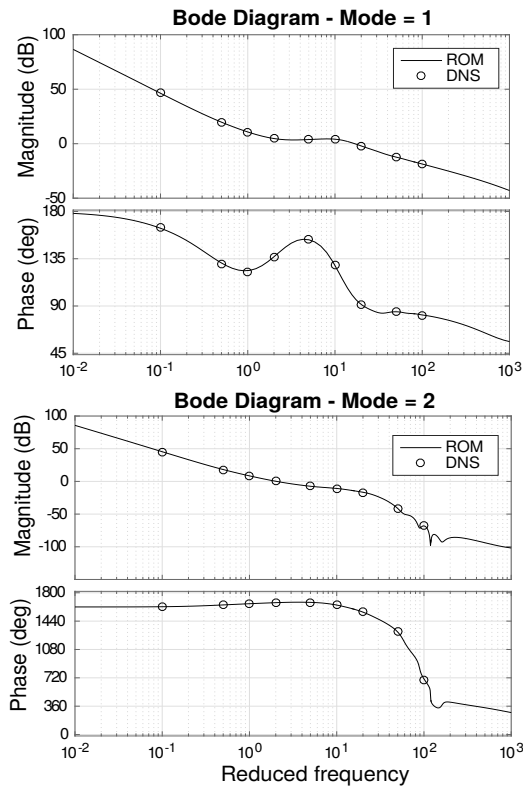
Figure 3: Frequency response of reduced order models for deflection modes 1 and 2 and comparison with DNS results.

of the wing at different time intervals and the lift comparison between model and DNS are also shown.

Conclusions

A linear reduced-order model that represents the lift generated by the unsteady deflection of a two-dimensional wing has been presented. High-fidelity DNS has been used together with system identification techniques to determine the coefficients of the reduced order model for single deflection modes. The magnitude of the lift pulse response decreases as the mode number k increases, showing a lower contribution to lift for higher modes and thus justifying the representation of the wing deflection with a truncated Fourier series. The accuracy of the reduced order model has been investigated, showing comparisons with DNS. The characteristics of the reduced order models have been discussed in the context of feedback control, posing new challenges for future work. Specifically, odd modes generate an inverse high-frequency response, while even modes show a time delay in the lift response. Both phenomena represent performance limitations from a control point of view.

References

[1] Brunton, S. L., Dawson, S. T. M. and Rowley, C. W., State-space model identification and feedback control of unsteady aerodynamic forces, *Journal of Fluids and Structures*, **50**, 2014, 253–270.

[2] Brunton, S. L. and Rowley, C. W., Unsteady aerodynamic models for agile flight at low Reynolds numbers, *New Horizons*, **0552**, 2010, 1–12.

[3] Eldredge, J. D., Wang, C. and Ol, M. V., A computational study of a canonical pitch-up, pitch-down wing maneuver, *AIAA paper*, **70**, 2009, 3242–3250.
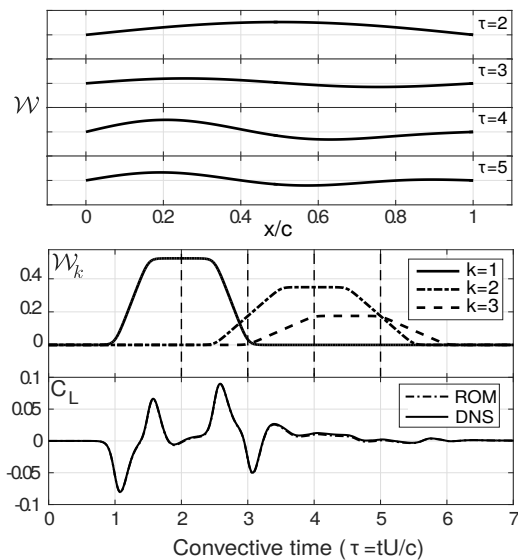
Figure 4: Combination of modes 1, 2 and 3, using the maneuver of equation (6) for each mode. The lift output of the reduced order model is compared to the lift obtained with DNS.

[4] Galiano, S. S. and Sandberg, R. D., Direct Numerical Simulations of Membrane Wings at Low Reynolds Number, in *53rd AIAA Aerospace Sciences Meeting*, 2015, AIAA SciTech, (AIAA 2015-1300).

[5] Juang, J.-N. and Pappa, R. S., An eigensystem realization algorithm for modal parameter identification and model reduction, *Journal of Guidance*, **8**, 1985, 620–627.

[6] Kang, C.-K., Aono, H., Cesnik, C. E. S. and Shyy, W., Effects of flexibility on the aerodynamic performance of flapping wings, *J. Fluid Mech*, **689**, 2011, 32–74.

[7] Leishman, J. G., Challenges in Modeling the Unsteady Aerodynamics of Wind Turbines, *21st ASME Wind Energy Symposium and the 40th AIAA Aerospace Sciences Meeting*, 1–28.

[8] Leishman, J. G., *Principles of Helicopter Aerodynamics*, Cambridge Aerospace Series, Cambridge University Press, 2002.

[9] Ma, Z., Ahuja, S. and Rowley, C. W., Reduced-order models for control of fluids using the eigensystem realization algorithm, *Theoretical and Computational Fluid Dynamics*, **25**, 2011, 233–247.

[10] Schlanderer, S. C. and Sandberg, R. D., Boundary Data Immersion Method for DNS of aero-vibro-acoustic systems, *ERCOFTAC Workshop Direct and Large-Eddy Simulations 10*.

[11] Schlanderer, S. C., Weymouth, G. and Sandberg, R., The Boundary Data Immersion Method for Compressible Flows with Application to Aeroacoustics, *Journal of Computational Physics, under review*.

[12] Shyy, W., Lian, Y., Tang, J., Liu, H., Trizila, P., Stanford, B., Bernal, L., Cesnik, C., Friedmann, P. and Ifju, P., Computational aerodynamics of low Reynolds number plunging, pitching and flexible wings for MAV applications, *Acta Mechanica Sinica/Lixue Xuebao*, **24**, 2008, 351–373.